

Behavior of a Meniscus Subjected to Transient Accelerations for Increasing Capillary Numbers

Kirk L. Yerkes*

U.S. Air Force Wright Laboratory, Wright–Patterson Air Force Base, Ohio 45433-7251
and

Kevin P. Hallinan†

University of Dayton, Dayton, Ohio 45469-0210

This study experimentally and analytically investigates the effects of acceleration transients on the dynamic response of an unheated meniscus in a capillary tube. A capillary tube partially filled with ethyl alcohol was mounted on a centrifuge to observe the dynamic response of the meniscus subject to single and multiple cycle acceleration transients. Experimental data of the meniscus recession and advance agreed well with a one-dimensional equation of motion accounting for changes in the receding and advancing contact angle assuming a spherically shaped meniscus. Systems typified by a low Bond number, as distinguished by a small capillary tube diameter, tended to be insensitive to transverse acceleration components. It was found that the combined effects of a Bond number less than 1.5 (distinguished by a small capillary tube diameter), and capillary number greater than 10^{-5} resulted in a retardation of the meniscus position, relative to the inviscid solution, due to acceleration transients. An additional retardation in the advancing meniscus position appeared to be due to an increase in the advancing contact angle with increasing capillary number.

Nomenclature

a	= capillary tube radius
B	= coefficient defined by Eqs. (4) and (5)
Bo	= Bond number, $(2a)^2 g_{pk} \rho / \sigma$
\vec{b}	= acceleration vector
Ca	= capillary number, $\mu V_c / \sigma$
\hat{e}	= unit vector
F_{s_z}	= surface force, axial component
f	= frequency of angular velocity
g	= gravitational acceleration
g_{pk}	= peak radial acceleration component
h_0	= static wicking height, $2\sigma \cos \theta / \rho a g \sin \phi$
Re	= Reynolds number, $(2a)\rho V_c / \mu$
r	= radial coordinate
r'_0	= radial location of capillary tube pivot point
t	= time
tf	= angular velocity cycle period, $1/f$
V_c	= characteristic velocity, $2h_0/tf$
We	= Weber number, $Re \times Ca$
z	= capillary tube axial directional coordinate
z_1	= capillary tube axial pivot location
ζ	= dimensionless meniscus position, η/h_0
η	= meniscus position
Θ	= dimensionless time, t/tf
θ_d	= recession or advancing contact angle
θ_s	= static contact angle
μ	= dynamic viscosity
ρ	= density
σ	= surface tension
τ_w	= wall shear stress
ϕ	= inclination angle
Ω	= angular velocity as a function of Θ
ω	= angular velocity

Subscripts

R	= capillary tube transverse direction
r_r	= centrifuge radial direction
s	= surface
T	= centrifuge tangential direction
y	= vertical direction
z	= capillary tube axial direction

Introduction

DEVICES such as heat pipes and capillary-pumped loops as well as many industrial processes (e.g., adhesive and lubrication technologies) utilize contact lines and capillarity to enhance heat and mass transfer. Heat pipe and capillary-pumped loop devices make use of condensation and evaporation processes associated with a wetting liquid on planar surfaces and within wicking structures consisting of porous media, grooved structures, and screens. The static and dynamic behavior of two- and three-phase contact lines ultimately dictates the effective performance of such devices in transporting heat and mass.

Additional difficulties arise when devices incorporating these processes are subjected to elevated steady-state and transient acceleration fields. Elevated steady-state acceleration fields resulting in forces on the same order of magnitude or greater than surface tension forces (more properly, the adhesion forces between the liquid and solid in the vicinity of the near contact line region) may affect the shape of the fluid interface. Transient acceleration-induced forces (both transverse and axial), in addition to altering the fluid interface shape, will cause motion of the contact line as the gravitational potential associated with the partially liquid-filled pore or groove changes. In such instances, the contact line velocity is functionally dependent on these transient acceleration-induced forces as well as surface tension. The inclusion of these elevated steady-state and transient acceleration fields defines a class of problems that are unique in the study of the static and dynamic behavior of contact lines.

Several macroscopic approaches have been used to describe the dynamics associated with an advancing or receding meniscus.^{1–4} In the macroscopic approach, the details of the near contact line region are ignored. Elliott and Riddiford¹ and

Received Nov. 9, 1994; revision received Feb. 21, 1995; accepted for publication Feb. 22, 1995. This paper is declared a work of the U.S. Government and is not subject to copyright protection in the United States.

*Research Engineer, WL/POOS-3, Aero Propulsion and Power Directorate.

†Associate Professor, Department of Mechanical Engineering.

Phillips and Riddiford² investigated the advancing and receding contact angle for a growing bubble between two flat plates as a function of interfacial velocity. They found a definitive relationship between the advancing or receding contact angle on interfacial velocity. For single liquid systems spreading on a dry surface, the advancing contact angle was found to be independent of the velocity for interfacial velocities up to 1 mm/min. For interfacial velocities greater than 1 mm/min, the advancing contact angle increased linearly to a limiting value. Qualitative molecular considerations were used to explain the velocity dependence of advancing contact angles. Relaxation of the contact angle from a dynamic value to a static value, when the fluid drive system was removed, was described as a molecular reorientation of the liquid molecules at the contact line.

Hoffman³ investigated the shape of an advancing interface in a capillary tube for which viscous and interfacial forces are the dominant salient features defining the system. He found a relationship between the advancing contact angle and the capillary number ($Ca = \mu V / \sigma$), plus a shift factor determined by the static contact angle.

Recently, Calvo et al.⁴ examined the advancing meniscus in a horizontal capillary tube attached to a liquid reservoir. It was found that the advance of the meniscus was controlled by the gravity head of the liquid above the capillary tube and the line force associated with the apparent contact line equal to $(2\sigma/a)\cos\theta_a$, where θ_a is the apparent contact line angle for dynamic conditions. Their results indicated that for capillary numbers less than 10^{-5} , $\theta_a \approx \theta_s$, the static contact angle. With increasing capillary numbers the dynamic contact angle increases for advancing menisci and decreases for receding menisci. The macroscopic predictions of the advancing rate of the meniscus showed good agreement with experimental data.

In general, prior investigations with regard to the dynamic behavior of the contact line have specified a contact line velocity consistent with a moving solid boundary or the steady forcing of a fluid using a drive system. There has been limited research with regard to the effects of acceleration-induced forces. Most of these have addressed the equilibrium free-surface shape.⁵ Yerkes and Hallinan⁶ discussed the dynamic behavior of the meniscus and contact line region in a capillary tube subject to a transient acceleration field for large Bond numbers. The transient acceleration-induced forces strictly controlled the contact line dynamics. Supported by experimental results and analytical calculations, they found that the combination of a decreasing Bond number, characterized by a small diameter capillary tube, and an increasing capillary number, $Ca > 10^{-5}$, resulted in the dynamic response of the meniscus consisting of an increase in the viscous retardation in meniscus position due to an acceleration transient. In addition, transverse acceleration components tended to alter the dynamic behavior of the meniscus as a result of reorienting the meniscus in the transverse direction and distending it in the axial direction.

It is the purpose of this article to experimentally and analytically expand the previous work describing the dynamic response of the meniscus in a capillary tube as a result of a single and multiple cycle acceleration transients. In particular, this article discusses the effects of a low Bond number less than 1.5 and capillary number greater than 10^{-5} for a system in which viscous, interfacial, and acceleration-induced forces control the motion of the meniscus.

Experimental

Acceleration Field

Transient acceleration fields were generated using a 2.4-m-diam centrifuge table (Fig. 1) rotating with a time variant angular velocity. Angular velocity transients were generated at a specified cyclic frequency, $0.0015 \text{ Hz} \leq f \leq 0.10 \text{ Hz}$, using a signal or waveform generator as a control input to the

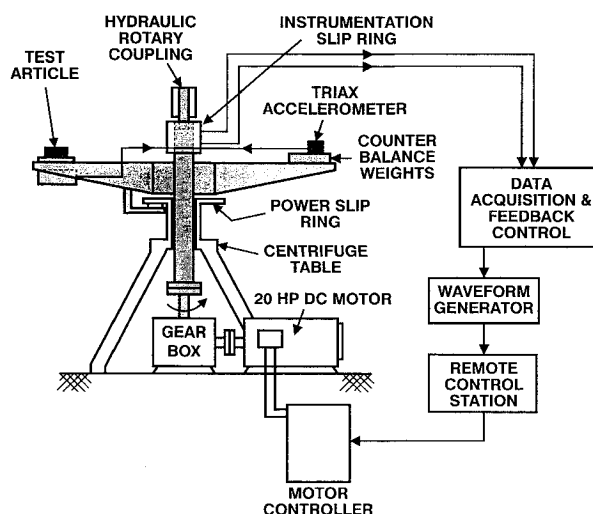


Fig. 1 Schematic of centrifuge.

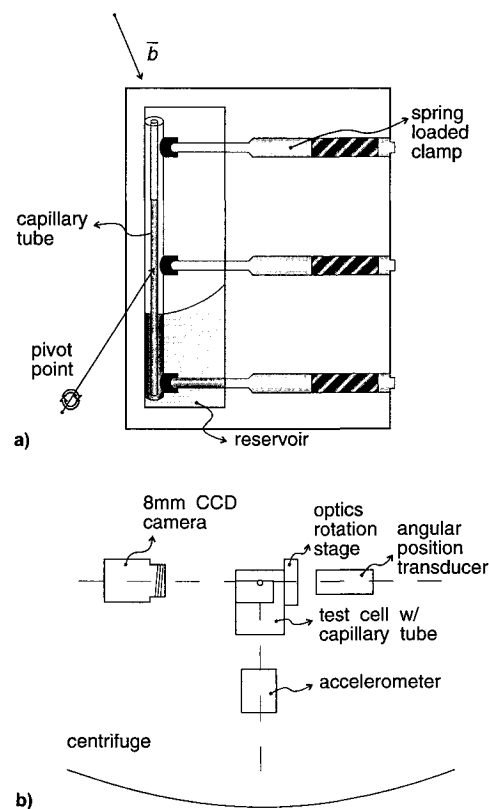


Fig. 2 Experimental apparatus: a) sealed test cell and b) schematic of experimental apparatus as mounted on the centrifuge.

centrifuge. The angular velocity was increased linearly to a peak value at the midpoint of the cycle and subsequently decreased for single and multiple cycles. A tri-axis accelerometer (Columbia Research Laboratories, Inc.) was used to monitor the time variant acceleration components in a Cartesian reference frame affixed to the centrifuge table. For this investigation, the peak angular velocity was specified such that a $4.2 g \pm 0.1 g$ peak radial acceleration was generated ($g_{pk} = 41.20 \text{ m/s}^2$).

Capillary Test Cell

A sealed test cell containing a glass capillary tube and reservoir was positioned on the centrifuge as shown in Fig. 2. The test cell was mounted to a motorized optics rotation stage (Newport) such that the capillary tube was allowed to pivot

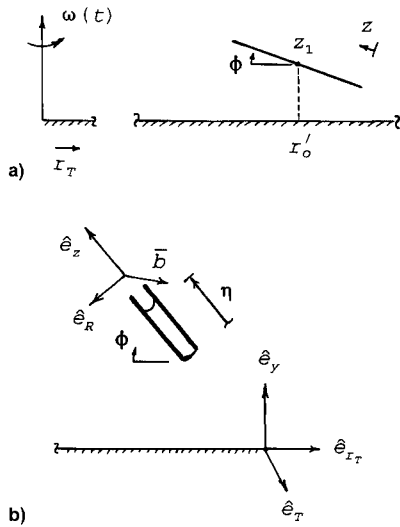


Fig. 3 Capillary tube orientation: a) pivot point location, directional coordinates and b) coordinate systems as referenced to the centrifuge accelerometer and capillary tube.

about its c.m. This pivot point was displaced vertically from the centrifuge surface at a fixed radial location r'_0 , as shown in Fig. 3a. Angles of inclination of the capillary tube were determined from the output of a calibrated angular position transducer (Trans-Tek, Inc.), accurate to within ± 0.2 deg.

Experiments were conducted by fixing the capillary tube at a specified inclination angle while subjecting it to the transient acceleration field. Increasing the inclination angle elevates the transverse acceleration component referenced to the capillary tube. This allowed the dynamic response of the meniscus subjected to an increasing transverse acceleration component to be observed experimentally. The dynamic response of the meniscus to the transient acceleration field was observed using an 8-mm format charge-coupled device (CCD) camera (Sony, 30 frames/s), mounted adjacent to the test cell as shown in Fig. 2b. Video images were used to provide a record of the meniscus height relative to the reservoir meniscus η , as a function of time to within ± 1.0 mm. A static contact angle θ_s was calculated from the experimentally determined static wicking height h_0 for conditions when the transverse acceleration component was zero [$h_0 \rho g \approx (2\sigma/a) \cos \theta_s$].

Ethyl alcohol was used as the test fluid to demonstrate the importance of the equilibrium contact angle on the advance and recession of the meniscus due to a transient acceleration field for low Bond numbers. Two capillary tubes, 1.0 and 0.5 mm in diameter, were used in order to vary the experimental Bond number. Properties of the ethyl alcohol were assumed to be that of the bulk fluid corresponding to an experimental temperature of 30°C.

The test cell and capillary tube were cleaned using potassium hydroxide and thoroughly rinsed with ethyl alcohol. The test cell was filled and subsequently sealed, resulting in a fill that had a combination of air, fluid vapor, and liquid.

Analytical Formulation

The goals of the analytical formulation were to expand the mathematical formulation described by Yerkes and Hallinan⁶ as follows:

1) Mathematically describe the dynamic behavior of the meniscus as a result of the temporal acceleration-induced forces using a simplified one-dimensional model with a constant line force accounting for changes in the recession and advancing contact angles.

2) Determine the relative importance of the transverse acceleration component and capillary number for low Bond numbers on the meniscus motion by comparing experimental results and analytical calculations.

Acceleration Vector

Acceleration measurements were obtained with regard to a three-dimensional Cartesian noninertial reference frame affixed to the centrifuge as described by Yerkes and Hallinan.⁶ The acceleration field was then referenced to fixed locations on the capillary tube and subsequently decomposed into transverse and axial acceleration components relative to the capillary tube as shown in Fig. 3b.

The resulting transient acceleration vector decomposed into an axial component b_z and a transverse component b_R , becomes

$$\begin{aligned} \bar{b} = & \{-\omega^2[r'_0 + (z_1 - z)\cos \phi]\cos \phi + (-g)\sin \phi\}\hat{e}_z \\ & + \left\{ \{-\omega^2[r'_0 + (z_1 - z)\cos \phi]\sin \phi - (-g)\cos \phi\}^2 \right. \\ & \left. + \left\{ [r'_0 + (z_1 - z)\cos \phi] \frac{d\omega}{dt} \right\}^2 \right\}^{1/2} \hat{e}_R \end{aligned} \quad (1)$$

Here, the transverse component b_R is a magnitude with no reference to direction due to the axisymmetric nature of the capillary tube. This form of the acceleration vector does not include the Coriolis acceleration that would be embodied in the transverse acceleration component. The Coriolis acceleration is induced from the motion of the fluid column or meniscus in the axial direction in the capillary tube. Therefore, prior knowledge of the meniscus dynamics, specifically the velocity, is required to evaluate the Coriolis acceleration. The one-dimensional equation of motion for the meniscus formulated for this investigation assumes that the transverse acceleration component has a negligible effect on the dynamic behavior of the meniscus, and therefore, does not account for tangential and Coriolis acceleration effects.

Equation of Motion

A simple analytical model described by Yerkes and Hallinan⁶ was used to predict the motion of the meniscus subjected to transient accelerations. The analytical formulation of the equation of motion was simplified assuming bulk flow only in the axial direction of the capillary tube.

The surface force F_{s_z} was formulated by accounting for the cumulative effect of solid-liquid intermolecular forces in the near contact line region and the wall shear stress associated with the predominantly Poiseuille flow in the liquid column. This approach has been used since the work of West⁷ and Washburn,⁸ and as described by Kafka and Dussan,⁹ has been surprisingly good in modeling steady capillary flows when Ca and Re are small. The contact line force is defined assuming a spherical meniscus and a constant apparent contact angle such that

$$F_{s_z} = \sigma(2\pi a)\cos \theta_s + \tau_w(2\pi a)\eta \quad (2)$$

Note that such an assumption implies a nonchanging apparent contact angle under dynamic conditions ($\theta_d \approx \theta_s$).

The resulting dimensional form of the momentum equation is

$$\begin{aligned} \frac{2\sigma \cos \theta}{\rho a} = & \left[\eta \frac{d^2 \eta}{dt^2} + \left(\frac{d\eta}{dt} \right)^2 \right] + \left(\frac{8\mu}{\rho a^2} \eta \frac{d\eta}{dt} \right) \\ & + \eta \left\{ \omega(t)^2 \cos \phi \left[\left(z_1 - \frac{\eta}{2} \right) \cos \phi + r'_0 \right] + g \sin \phi \right\} \end{aligned} \quad (3)$$

The transient angular velocity is of the form

$$\begin{aligned} \omega(t) = & Bt, \quad 0 \leq t \leq (tf/2) \\ = & B(tf - t), \quad (tf/2) \leq t \leq tf \end{aligned} \quad (4)$$

where

$$B = \left[\frac{4g_{pk}}{(tf)^2 r_0'} \right]^{1/2} \quad (5)$$

Using the following dimensionless parameters:

$$\begin{aligned} \zeta &= \eta/h_0, & 0 \leq \zeta \leq 1 \\ \Theta &= t/tf, & 0 \leq \Theta \leq 1 \end{aligned} \quad (6)$$

with the following initial conditions:

$$\zeta = 1, \quad \frac{d\zeta}{d\Theta} = 0, \quad \Theta = 0$$

the nondimensional form of the momentum equation in terms of a transient dimensionless meniscus position becomes

$$\begin{aligned} \frac{g}{g_{pk}} \sin \phi &= \left(\frac{a}{h_0} \right) \left(\frac{ReCa}{2Bo} \right) \left[\zeta \frac{d^2\zeta}{d\Theta^2} + \left(\frac{d\zeta}{d\Theta} \right)^2 \right] \\ &+ \left(\frac{16Ca}{Bo} \right) \left(\zeta \frac{d\zeta}{d\Theta} \right) + \zeta \left\{ \Omega(\Theta)^2 \cos \phi \right. \\ &\times \left[\left(z_1 - \frac{h_0\zeta}{2} \right) \cos \phi + r_0' \right] + \frac{g}{g_{pk}} \sin \phi \left. \right\} \end{aligned} \quad (7)$$

where the angular velocity Ω is defined by

$$\begin{aligned} \Omega(\Theta) &= (4/r_0')^{1/2} \Theta, & 0 \leq \Theta \leq \frac{1}{2} \\ &= (4/r_0')^{1/2} (1 - \Theta), & \frac{1}{2} \leq \Theta \leq 1 \end{aligned} \quad (8)$$

The first and second terms of Eq. (7) represent the inertial and viscous effects, respectively, with the coefficients formed as the products of the Reynolds number, capillary number, Bond number, and aspect ratio. The Reynolds and capillary numbers are referenced to a characteristic velocity V_c , which is the maximum attainable velocity over one-half of the acceleration cycle period assuming $\eta = 0$ at g_{pk} . The Bond number is referenced to the peak radial acceleration component g_{pk} .

The momentum equation can be easily modified to include a constant receding or advancing contact angle θ_d , differing from that of the static contact angle θ_s , resulting in

$$\begin{aligned} \frac{g}{g_{pk}} \frac{\cos \theta_d}{\cos \theta_s} \sin \phi &= \left(\frac{a}{h_0} \right) \left(\frac{ReCa}{2Bo} \right) \left[\zeta \frac{d^2\zeta}{d\Theta^2} + \left(\frac{d\zeta}{d\Theta} \right)^2 \right] \\ &+ \left(\frac{16Ca}{Bo} \right) \left(\zeta \frac{d\zeta}{d\Theta} \right) + \zeta \left\{ \Omega(\Theta)^2 \cos \phi \right. \\ &\times \left[\left(z_1 - \frac{h_0\zeta}{2} \right) \cos \phi + r_0' \right] + \frac{g}{g_{pk}} \sin \phi \left. \right\} \end{aligned} \quad (9)$$

It may be noted that the general form of the dynamic contact angle is known to be functionally dependent on the contact line receding and advancing velocity, $\theta_d = \theta_d(d\zeta/d\Theta)$, as discussed by Jiang et al.¹⁰ for the data presented by Hoffman.³ Equation (9) can be modified to include any specific form for the dynamic contact angle and solved numerically.

Results

Equation (9) was solved for the dimensionless meniscus position ζ using a central difference scheme. Solutions were obtained by first specifying a static wicking height h_0 based on the experimentally determined static contact angle $\theta_s = 16.7$ deg. Numerical solutions were consistent with the experimental parameters for $Bo = 0.3675$, 1.47 , and $3.47 \times$

$10^{-6} \leq Ca \leq 4.00 \times 10^{-4}$ with single or multiple acceleration transient cycles. Numerical solutions were also calculated for various advancing contact angles in order to address deviations between experimental results and analytical calculations based upon the assumption that the contact angle is equivalent to the static contact angle θ_s . All numerical solutions assumed a constant recession contact angle equivalent to the static contact angle, $\theta_d = \theta_s = 16.7$ deg.

Experiments were performed and the results compared with solutions to the analytical model. Uncertainty in the experimentally obtained dimensionless meniscus position ζ and time Θ was on the order of $\zeta, \Theta \pm 0.02$, based on the accuracy and resolution of experimentally measured quantities.

Figure 4 compares the experimentally obtained dimensionless meniscus position to the analytical results at varying angles of inclination for small capillary numbers, assuming the recession and advancing contact angle are equivalent to the static contact angle. Also shown are the axial and transverse acceleration components. Experimental parameters in this figure ranged from $3.47 \times 10^{-6} \leq Ca \leq 6.00 \times 10^{-6}$, $2.96 \times 10^{-2} \leq Re \leq 5.13 \times 10^{-2}$, and $5.71 \times 10^{-3} \leq a/h_0 \leq 9.89 \times 10^{-3}$ for inclination angles of 30 and 60 deg. The experimentally obtained dimensionless meniscus position agreed well with the analytical calculations. There was a slight deviation for the 60-deg inclination angle from the predicted values due to an increase in the transverse acceleration component as shown in Fig. 4b, as was observed by Yerkes and Hallinan.⁶ Relative to the previous work,⁶ a small Bond number tended to decrease the sensitivity of the meniscus position to the transverse acceleration component.

Figure 5 compares the experimental results and analytical calculations for $4.00 \times 10^{-5} \leq Ca \leq 4.00 \times 10^{-4}$ with $Bo = 1.47$ at 25-deg inclination and $Bo = 0.3675$ at 30-deg in-

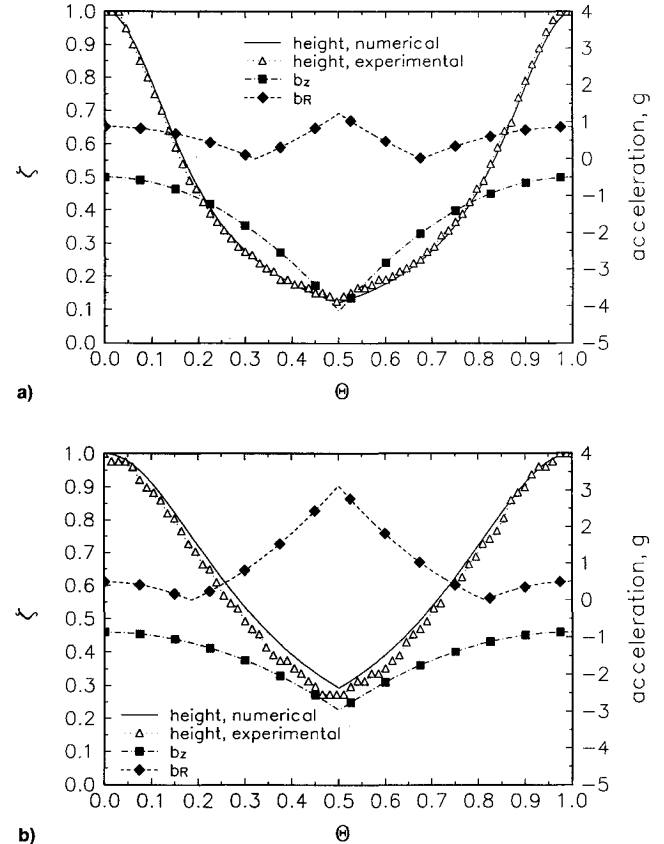
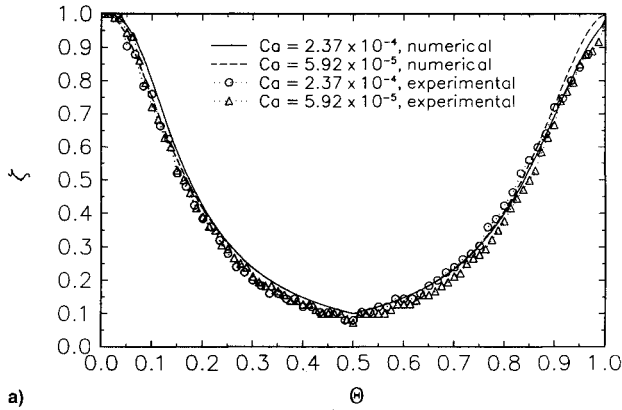


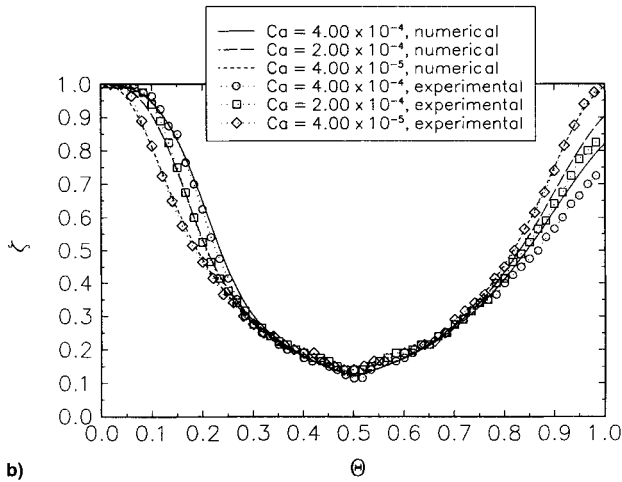
Fig. 4 Experimental data compared to analytical calculations for ethyl alcohol at $Bo = 0.3675$ ($\theta_d = \theta_s = 16.7$ deg): a) $\phi = 30$ deg, $Ca = 6.00 \times 10^{-6}$, $Re = 5.13 \times 10^{-2}$, $a/h_0 = 5.71 \times 10^{-3}$ and b) $\phi = 60$ deg, $Ca = 3.47 \times 10^{-6}$, $Re = 2.96 \times 10^{-2}$, $a/h_0 = 9.89 \times 10^{-3}$.

Table 1 Values of dimensionless numbers

Bo	Ca	Re	We	al/h_0	ϕ , deg
0.3675	4.00×10^{-4}	3.42	1.37×10^{-3}	5.71×10^{-3}	30
	2.00×10^{-4}	1.71	3.42×10^{-4}	—	
	1.00×10^{-4}	0.855	8.55×10^{-5}	—	
	4.00×10^{-5}	0.342	1.37×10^{-5}	—	
	6.00×10^{-6a}	5.13×10^{-2}	3.08×10^{-7}	—	
1.47	2.37×10^{-4}	4.05	9.60×10^{-4}	1.93×10^{-2}	25
	1.18×10^{-4}	2.02	2.38×10^{-4}	—	
	5.92×10^{-5}	1.01	5.98×10^{-5}	—	
	3.55×10^{-6b}	6.07×10^{-2}	2.15×10^{-7}	—	

^aFig. 4a. ^bYerkes and Hallinan.⁶

a)

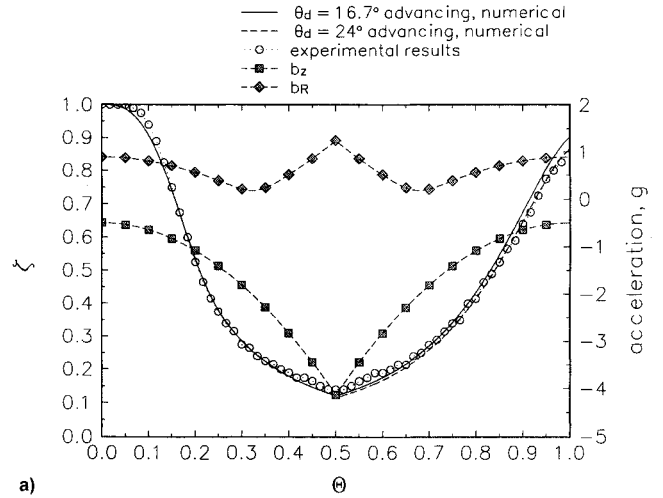


b)

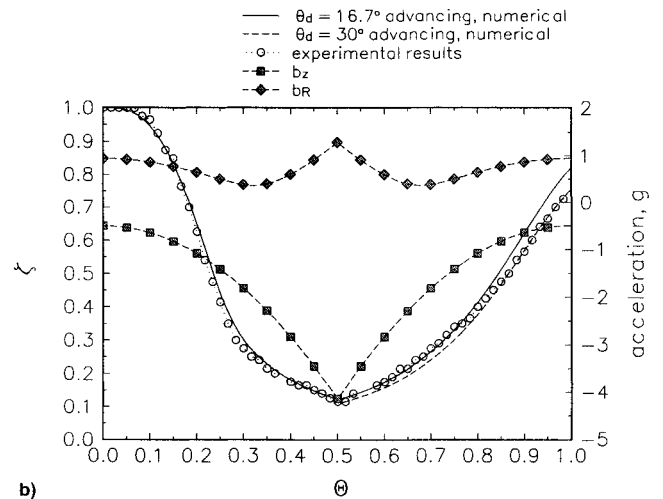
Fig. 5 Experimental data compared to analytical calculations for varying capillary number ($\theta_a = \theta_r = 16.7$ deg): a) $\phi = 25$ deg, $Bo = 1.47$ and b) $\phi = 30$ deg, $Bo = 0.3675$.

clination, assuming the recession and advancing contact angle are equivalent to the static contact angle. Table 1 shows a summary of the dimensionless parameters corresponding to Fig. 5.

As shown in Fig. 5a, there was no significant deviation between the predicted and observed meniscus position for $Bo = 1.47$. For $Bo = 0.3675$, as shown in Fig. 5b, the predicted and observed meniscus position agreed well for meniscus recession, with an increase in the retardation in meniscus position corresponding to an increase in the capillary number. For the advancing meniscus, there was a retardation in the observed meniscus position, in response to the acceleration transient, from that of the predicted values. The retarded position for the advancing meniscus was not evident for $Ca = 4.00 \times 10^{-5}$, but was significant for higher capillary numbers with an increase in retardation as the capillary number increased.



a)



b)

Fig. 6 Experimental data compared to analytical calculations for varying advancing contact angle, $\phi = 30$ deg, $Bo = 0.3675$ (16.7-deg receding contact angle) and acceleration field. $Ca =$ a) 2.00×10^{-4} and b) 4.00×10^{-4} .

The variation between the predicted and observed advancing meniscus velocity is in part due to the dependence of the contact angle on capillary number and/or Reynolds number. Figure 6 compares the analytical calculations for a 16.7-deg receding contact angle while varying the advancing contact angle. Also shown in Fig. 6 are the transient acceleration fields decomposed into the axial and transverse components at the pivot point of the capillary tube. The experimental results agree very well with that of the analytical calculations when a change in the advancing contact angle is taken into account.

Hoffman³ and Phillips and Riddiford² discuss systems in which the interfacial forces between the solid and the liquid change when flow occurs under conditions where inertia is

assumed to be negligible. For very low velocities the apparent contact angle is usually independent of velocity, but as the interfacial velocity is increased above a critical velocity, the apparent contact angle will change until a limiting value is reached. Phillips and Riddiford postulated that there is a change in the interfacial forces as the critical velocity is reached, thereby resulting in a shift in the apparent contact angle. Figures 6a and 6b show that the advancing velocity agrees well with the analytical calculations up to $\Theta \approx 0.75$, corresponding to an inflection in the transverse acceleration component. The meniscus velocity at $\Theta \approx 0.75$ suddenly decreases (from ≈ 3 mm/s for $Ca = 2.00 \times 10^{-4}$ and ≈ 6 mm/s for $Ca = 4.00 \times 10^{-4}$), and subsequently increases again, resulting in a retarded meniscus position compared to the analytical solution. The sudden decrease in the meniscus velocity at time $\Theta \approx 0.75$ and subsequent increase may be due to the combined effects of the transverse acceleration component and the Coriolis acceleration, which is dependent on the velocity of the meniscus. The analytical formulation takes into account the opposing viscous force at the tube wall and general inertial effects, but does not take into account the opposing viscous force at the contact line region and a possible increase in the radius of curvature of the meniscus as a result of inertial effects. Analytical calculations and experimental results show that the motion of the meniscus along the contact line and fluid along the tube wall is retarded due to viscous effects. However, the motion of the central core of fluid, due to inertia, likely results in the "pushing forward" of the central portion of the meniscus relative to the contact line, yielding an increased radius of curvature, and therefore, an increased contact angle. This change in contact angle further retards the meniscus motion.

In addition, with the removal of the acceleration transient, there is a rapid but noticeable relaxation time (≈ 4 – 5 s), when the contact angle returns to the static value and the column of alcohol returns to the initial static wicking height. The existence of a relaxation time agrees with observations by Phillips and Riddiford.

Figure 7 compares the analytically calculated advancing contact angle required to match experimental results to the results presented by Hoffman.³ The shifting function described by Hoffman was determined to be approximately $F(\theta_a) = 2.5 \times 10^{-4}$. Using a capillary number as defined in this investigation (really an average capillary number), $Ca + F(\theta_a)$ was plotted against the advancing contact angle. The deviation from that of Hoffman's results may be in part due to the fact that Hoffman is characterizing the shape of the liquid-air interface for viscous fluids (i.e., oils) in motion when only the viscous and interfacial forces are important. This investigation considers motion of the liquid-air interface for ethyl alcohol as a result of acceleration-induced forces where inertial, viscous, and interfacial forces are significant.

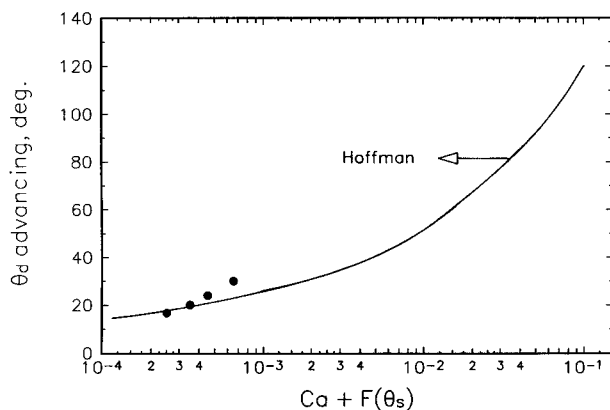


Fig. 7 Comparison of Hoffman's³ results and advancing contact angle required to match experimental results.

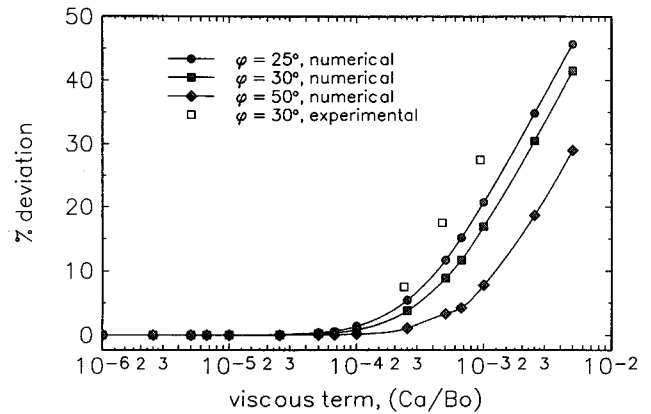


Fig. 8 Percent retardation from the inviscid solution at the end of a cycle.

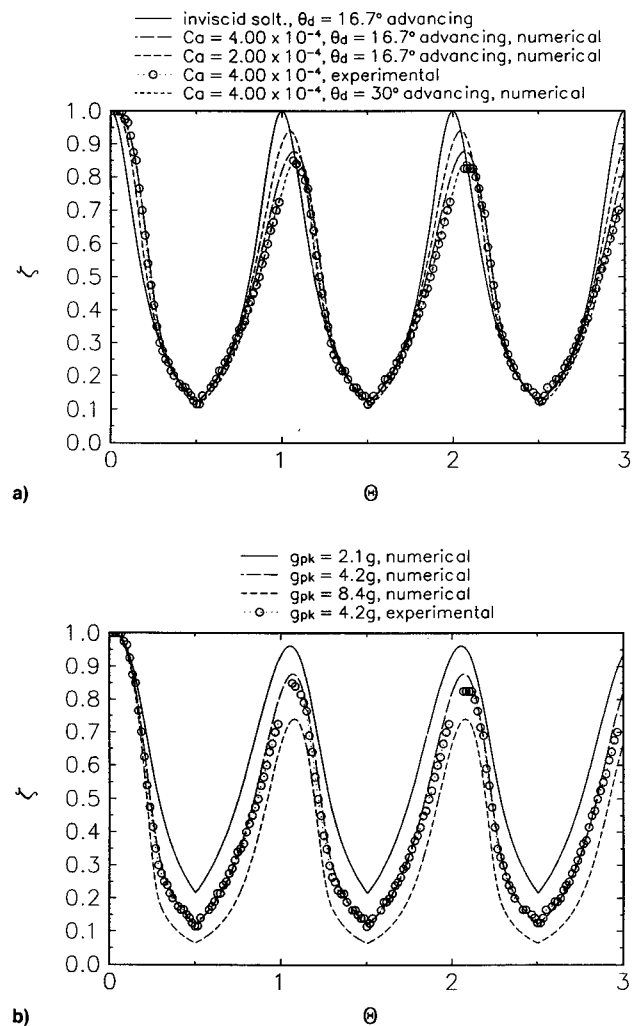


Fig. 9 Experimental data compared to analytical calculations for multiple acceleration cycles ($\phi = 30$ deg, $Bo = 0.3675$): a) varying capillary number, $g_{pk} = 4.2$ g and b) varying g_{pk} , $Ca = 4.00 \times 10^{-4}$.

Figure 8 shows the percent retardation in the meniscus position from the inviscid solution, at the end of a cycle, relative to the viscous term Ca/Bo . The effect of increasing the angle of inclination resulted in a reduction in the percent retardation from the inviscid solution since the meniscus velocity decreases with increasing inclination angle and viscous forces are therefore reduced. As shown in Fig. 8, the experimental results for a 30-deg inclination showed an increased retardation from the viscous analytical solutions based on a

fixed contact angle. This increase in the meniscus retardation between the experimental results and analytical predictions provides credibility to the hypothesis that inertial forces not included in the Ca/Bo number term may result in a change in the contact angle and that viscous forces alone are not sufficient to induce the observed increase in the retardation from the inviscid prediction.

Figure 9 compares analytical calculations and experimental results for three cycles in the transient acceleration for $Bo = 0.3675$, $Ca = 2.00 \times 10^{-4}$, and 4.00×10^{-4} , $g_{pk} = 2.1 g$, $4.2 g$, $8.4 g$, and at a 30-deg inclination angle. As shown in Fig. 9a, by varying the capillary number, there is an attenuation and phase shift in meniscus position due to viscous effects from an inviscid or low capillary number solution as the capillary number is increased. Again, there is good agreement between the observed and predicted receding meniscus position. The deviation between the observed and predicted advancing meniscus position is apparent, however, when an advancing contact angle of 30 deg is accounted for in the numerical solution. The predicted and observed meniscus positions agree very well. As shown in Fig. 9b, by varying the peak radial acceleration, there is an increased attenuation from the initial meniscus height and a slight phase shift with an increasing peak radial acceleration.

Concluding Remarks

The dynamic response of an unheated meniscus within a capillary tube subjected to single and multiple cycle transient acceleration-induced forces was demonstrated experimentally and analytically. Comparison of the experimental and analytical results showed, for systems typified by a low Bond number, a tendency to be less sensitive to transverse acceleration components due to the small capillary tube diameter. This, however, is not the case for larger Bond numbers as distinguished by the larger capillary tube diameters. For systems typified by the combination of a low Bond number and high capillary number, there was a significant change in the dynamic response of the meniscus due to the combination of viscous forces, acceleration-induced inertial forces, and interfacial forces. It may be noted that variations in either the receding contact angle or the advancing contact angle are indicative of changes in any or all of these forces described.

The practical significance of these results, as related to heat transfer devices utilizing contact lines and capillarity to enhance heat and mass transfer, has been to provide a better understanding of the physics and initial information helpful in extrapolating performance information for particular devices operating in the range of Bond and capillary numbers specified. Such heat transfer devices subjected to single and

multiple cycle acceleration transients, such as may be encountered aboard high-performance aircraft, may tend to deprime and reprime at rates dependent on the combination of Bond and capillary numbers defined by the capillary structure, acceleration transient amplitude and frequency, and working fluid. More importantly, even without heat addition, the meniscus may never reprime to the original state during these acceleration transients or be slow to reprime at the cessation of the acceleration transients due to variations in viscous, inertial, and interfacial forces. With the addition of heat, the deprime and reprime dynamics may be significantly altered and result in either a degraded or possibly improved performance such as with the arterial heat pipe discussed by Yerkes et al.¹¹

References

- ¹Elliott, G. E. P., and Riddiford, A. C., "Dynamic Contact Angles I. The Effect of Impressed Motion," *Journal of Colloid and Interface Science*, Vol. 23, 1967, pp. 389–398.
- ²Phillips, M. C., and Riddiford, A. C., "Dynamic Contact Angles II. Velocity and Relaxation Effects for Various Liquids," *Journal of Colloid and Interface Science*, Vol. 41, No. 1, 1972, pp. 77–85.
- ³Hoffman, R. L., "A Study of the Advancing Interface I. Interface Shape in Liquid-Gas Systems," *Journal of Colloid and Interface Science*, Vol. 50, No. 2, 1975, pp. 228–240.
- ⁴Calvo, A., Paterson, I., Chertcoff, R., Rosen, M., and Hulin, J. P., "Dynamic Capillary Pressure Variations in Diphasic Flows Through Glass Capillaries," *Journal of Colloid and Interface Science*, Vol. 141, No. 2, 1991, pp. 384–394.
- ⁵Concus, P., "Static Menisci in a Vertical Right Circular Cylinder," *Journal of Fluid Mechanics*, Vol. 34, 1968, pp. 481–495.
- ⁶Yerkes, K. L., and Hallinan, K. P., "Dynamic Behavior of an Unheated Meniscus Subjected to a Transient Acceleration Field," *Journal of Thermophysics and Heat Transfer*, Vol. 9, No. 2, 1995, pp. 322–328.
- ⁷West, G. D., "On Resistance to the Motion of a Thread of Mercury in a Glass Tube," *Proceedings of the Royal Society of London, Series A, Mathematical and Physical Sciences*, Vol. 86, 1911–1912, p. 20.
- ⁸Washburn, E. W., "The Dynamics of Capillary Flow," *Physical Review*, Vol. 17, 1921, pp. 273–283.
- ⁹Kafka, F. Y., and Dussan V., E. B., "On the Interpretation of Dynamic Contact Angles in Capillaries," *Journal of Fluid Mechanics*, Vol. 95, 1979, pp. 539–564.
- ¹⁰Jiang, T. S., Oh, S. G., and Slaterry, J. C., "Correlation for Dynamic Contact Angle," *Journal of Colloid and Interface Science*, Vol. 69, No. 1, 1979, pp. 74–77.
- ¹¹Yerkes, K. L., Chang, W. S., and Beam, J. E., "Heat Pipe Performance with Transient Heat Flux and Body Force Effects," *Advances in Heat Pipe Science and Technology, Proceedings of the 8th International Heat Pipe Conference* (Beijing, PRC), 1992, pp. 205–213.